

## Article

# Detection of Acetaminophen and Its Glucuronide in Fingerprint by SALDI Mass Spectrometry Using Zeolite and Study of Time-Dependent Changes in Detected Ion Amount

Toshiki Horikoshi <sup>1</sup>, Chihiro Kitaoka <sup>2</sup>, Yosuke Fujii <sup>3</sup>, Takashi Asano <sup>4</sup>, Jiawei Xu <sup>1,5</sup> and Tatsuya Fujino <sup>1,5,\*</sup>

<sup>1</sup> Department of Applied Chemistry, Graduate School of Science and Engineering, Toyo University, 2100 Kujirai, Kawagoe 350-8585, Japan; s36d02100226@toyo.jp (T.H.); xu@toyo.jp (J.X.)

<sup>2</sup> Criminal Investigation Laboratory, Metropolitan Police Department, 2-1-1 Kasumigaseki, Chiyoda-ku, Tokyo 100-8929, Japan; kitaoka-chihiro@outlook.jp

<sup>3</sup> Department of Chemistry, Graduate School of Science and Engineering, Tokyo Metropolitan University, 1-1 Minami-Osawa, Hachioji, Tokyo 192-0379, Japan; yosuke.fujii.221@gmail.com

<sup>4</sup> Forensic Science Laboratory, Metropolitan Police Department, 2-1-1 Kasumigaseki, Chiyoda-ku, Tokyo 100-8929, Japan; asanofam@dc.mbn.or.jp

<sup>5</sup> Bio-Nano Electronics Research Centre, Toyo University, 2100 Kujirai, Kawagoe 350-8585, Japan

\* Correspondence: fujino048@toyo.jp

**Abstract:** The ingredients of an antipyretic (acetaminophen, AAP) and their metabolites excreted into fingerprint were detected by surface-assisted laser desorption ionization (SALDI) mass spectrometry using zeolite. In the fingerprint taken 4 h after AAP ingestion, not only AAP but also the glucuronic acid conjugate of AAP (GAAP), caffeine (Caf), ethenzamide (Eth), salicylamide (Sala; a metabolite of Eth), and urea were detected. Fingerprints were collected over time to determine how the amounts of AAP and its metabolite changed with time, and the time dependence of the peak intensities of protonated AAP and GAAP was measured. It was found that the increase of [GAAP+H]<sup>+</sup> peak started later than that of [AAP+H]<sup>+</sup> peak, reflecting the metabolism of AAP. Both AAP and GAAP reached maximum concentrations approximately 3 h after ingestion, and were excreted from the body with a half-life of approximately 3.3 h. In addition, fingerprint preservation was confirmed by optical microscopy, and fingerprint shape was retained even after laser irradiation of the fingerprint. Our method may be used in fingerprint analysis.

**Keywords:** matrix-assisted laser desorption ionization (MALDI); surface-assisted laser desorption ionization (SALDI); fingerprint; acetaminophen; zeolite



**Citation:** Horikoshi, T.; Kitaoka, C.; Fujii, Y.; Asano, T.; Xu, J.; Fujino, T. Detection of Acetaminophen and Its Glucuronide in Fingerprint by SALDI Mass Spectrometry Using Zeolite and Study of Time-Dependent Changes in Detected Ion Amount. *Analytica* **2021**, *2*, 66–75. <https://doi.org/10.3390/analytica2030008>

Academic Editor: Marcello Locatelli

Received: 25 June 2021

Accepted: 28 July 2021

Published: 2 August 2021

**Publisher's Note:** MDPI stays neutral with regard to jurisdictional claims in published maps and institutional affiliations.



**Copyright:** © 2021 by the authors. Licensee MDPI, Basel, Switzerland. This article is an open access article distributed under the terms and conditions of the Creative Commons Attribution (CC BY) license (<https://creativecommons.org/licenses/by/4.0/>).

## 1. Introduction

Fingerprints are used to identify an individual because fingerprints are unique to each person and remain unchanged throughout one's life. In forensic investigation, fingerprint powder containing magnetic or metallic particles is generally used to visualize fingerprints [1]. Electric dust is attached to fingerprints in the first place. Fine particles such as silica contained in fingerprint powder electrostatically adhere to the electric dust, facilitating the visualization of fingerprints. Such fingerprint powder basically produces white and black patterns, but problems arise when fingerprints are on a substrate with multiple colors (such as banknotes) or with different smoothness. To prevent this, fluorescent fingerprint powders have also been developed [1,2].

Fingerprints can also help identify chemicals and metabolites excreted by sweat glands on fingertips. Gold or magnetic nanoparticles having antibody recognition properties are used to identify specific drugs or drug metabolites in fingerprints [3,4]. Mass spectrometry is a powerful tool for the identification of chemicals and metabolites in fingerprints. For example, gas chromatography mass spectrometry (GC-MS) was used to detect chemical changes in lipid component [5]. Liquid chromatography mass spectrometry (LC-MS) was

used to identify oxidation products of squalene [6], and methadone and its metabolites [7]. Matrix-assisted laser desorption/ionization (MALDI) [8–10], surface-assisted laser desorption/ionization (SALDI) [11], and desorption electrospray ionization (DESI) [12] were also used for imaging of fingerprints. Unfortunately, mass spectrometry has one drawback: as sample ionization is carried out, the sample is inevitably destroyed during measurement, leading to the loss of important fingerprint evidence. However, it was reported that the original fingerprint image could be restored even after MALDI mass measurements using  $\alpha$ -cyano-4-hydroxycinnamic acid (CHCA) used as matrix [13].

We report herein a method for detecting drugs in fingerprints by SALDI mass spectrometry. We would like to mention in particular that the drug in the fingerprint could be detected with high efficiency by using zeolite. Using CHCA adsorbed on the zeolite surface, fingerprints collected from multiple volunteers were measured. All volunteers took the same antipyretic, the main ingredients of which are acetaminophen (AAP), ethenzamide (Eth), and caffeine (Caf). Not only AAP but also its glucuronic acid conjugate (GAAP), Caf, Eth, and urea were detected. This method using CHCA adsorbed on zeolite was adopted in our previous study to detect drugs and metabolites in urine [14]. We collected the fingerprints over time to see how the drug and its metabolite in the fingerprints changed with time. As expected, the peak of metabolite GAAP appeared at a later time relative to that of AAP. By curve-fitting analysis, we estimated the time constants until the drug and its metabolite were excreted into sweat in the fingerprints. Finally, through optical microscopy, we confirmed whether fingerprint recovery is possible after the application of CHCA/zeolite.

## 2. Materials and Methods

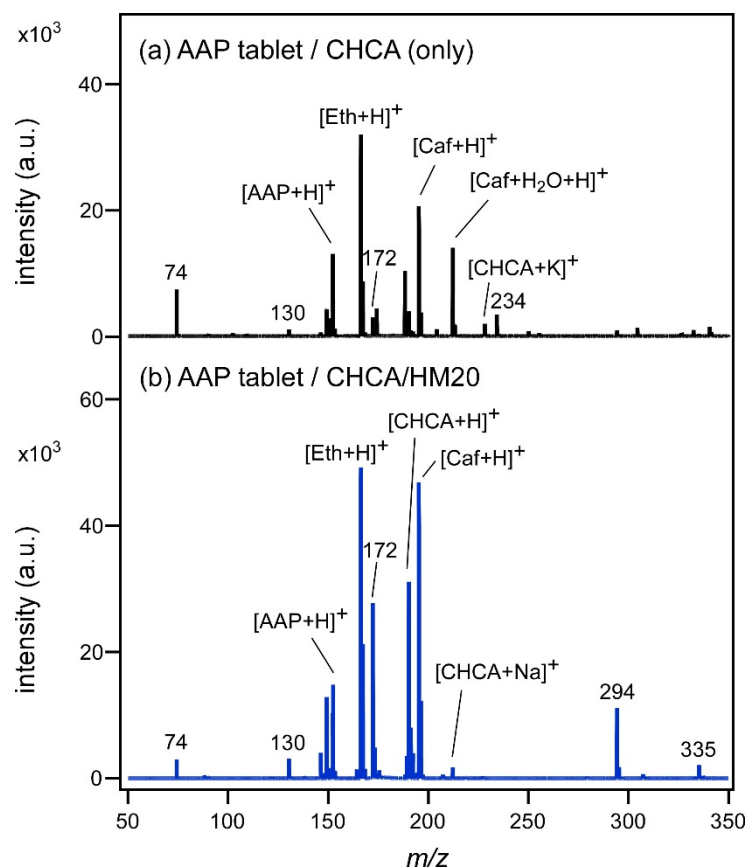
A CHCA ( $\alpha$ -cyano-4-hydroxycinnamic acid) solution (4 mg/mL) was used as the matrix solution for MALDI mass measurements. A mixture of acetonitrile and water (volume ratio 7:3) was used as the solvent. CHCA and zeolite (JRC-Z-HM20) were mixed in a mortar at the mass ratio of 1:2 and suspended in the mixed solvent of acetonitrile and water.

In this study, fingerprints collected from multiple volunteers who ingested a commercially available antipyretic due to such symptoms as headache were measured. Fingerprint samples were provided by the following procedure so that they would not be affected by anything other than the excretions from the fingertips. (1) The hands were washed with commercially available soap for 30 s. (2) The soap was rinsed off with tap water for 30 s. (3) The hands were wiped with dry paper towel for 30 s. (4) The fingertips were pressed against a stainless-steel sample plate for 30 s. (5) One microliter of CHCA matrix solution or CHCA/HM20 suspension was dropped onto the fingerprints. (6) After evaporating the solvent, the ions in the fingerprints were measured. Measurements were carried out by a commercial time-of-flight (TOF) mass system (MALDI micro MX<sup>TM</sup>, Waters, Milford, MA, USA) in the positive ion mode using a reflectron with a nitrogen laser operated at 337 nm and the excitation laser power of 5.9  $\mu$ J. Mass spectra were obtained by averaging 200 laser shots at random sample spots.

Microscopic images were taken using a commercially available inverted microscope (LEICA DMI8, Wetzlar, Germany). For the fingerprint preservation experiments, fingerprints were collected by pressing fingertip against a cover glass with a thickness of 0.12 mm to 0.17 mm (MATSUNAMI, 20  $\times$  30 mm) for 30 s. The CHCA/HM20 suspension was dropped onto the fingerprint, and the solvent was evaporated. An Nd:YAG laser (New Wave Research, Tempest, 266 nm, 10 Hz, 18  $\mu$ J) was used, and the output was focused by an  $f = 200$  quartz lens on the cover glass at random spots. After laser light irradiation, CHCA/HM20 was washed off by using a mixed solvent of acetonitrile and water (volume ratio 7:3) of 10 mL volume. After the solvent was dried, activated carbon powder (Wako) was sprinkled on the cover glass to visualize the fingerprint.

### 3. Results

Figure 1a shows the MALDI mass spectrum of 1 mg of AAP tablet measured by using CHCA as the matrix. AAP, Eth, and Caf, which are the main ingredients in the tablet, were observed as proton adducted ions. One tablet contains 150 mg of AAP, 80 mg of Eth, and 35 mg of caffeine hydrate ( $C_8H_{10}N_4O_2 \cdot H_2O$ ), and weighs of 0.3 g. Therefore, the amounts of AAP, Eth, and Caf used for the measurement in Figure 1a were calculated as 29.8, 14.5, and 4.53 nmol, respectively. Figure 1b shows the SALDI mass spectrum of AAP tablet measured by using CHCA/HM20, which was used for the subsequent fingerprint measurement. Even when CHCA/HM20 was used, the peaks of protonated AAP, Eth, and Caf were observed, as in the case of Figure 1a. Furthermore, the intensities of the peaks increased; AAP was increased by 1.14 times, Eth by 1.55 times, and Caf by 2.28 times. Therefore, it was clarified that such chemical substances as AAP, Eth, and Caf could be ionized effectively by SALDI using CHCA/HM20. The AAP tablet contains hydroxypropyl cellulose, calcium silicate,  $\alpha$ -starch, and magnesium stearate in addition to the above three ingredients. Therefore, some of the unknown peaks may have been derived from these substances. The  $m/z$  value, assignment, and intensity for each peak observed in Figure 1 were summarized in Table 1.



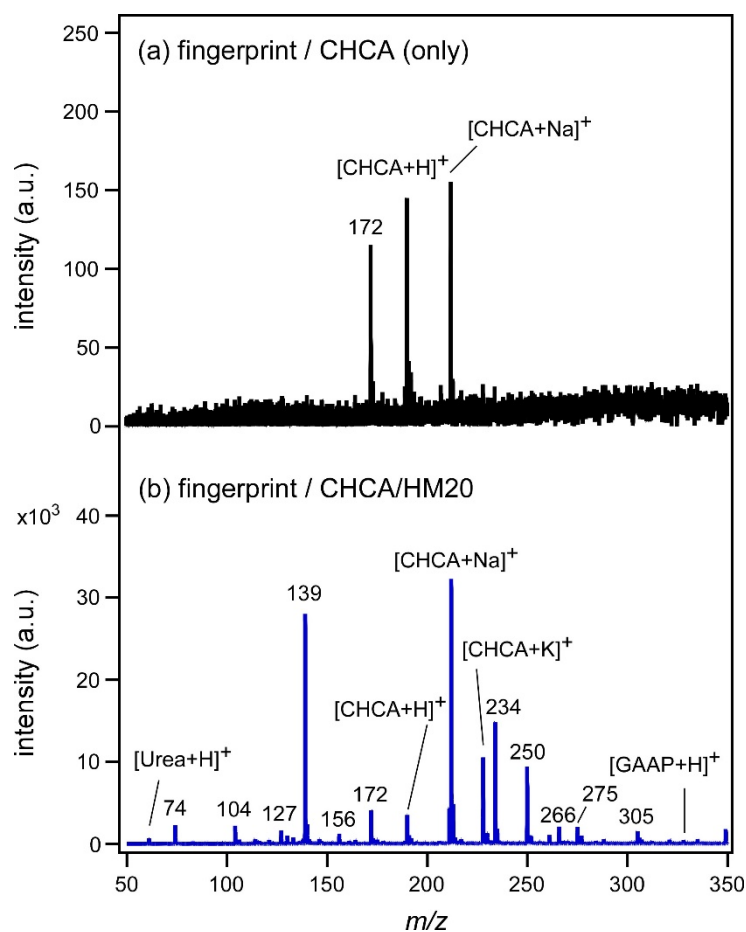
**Figure 1.** (a) MALDI mass spectrum of AAP tablet measured with CHCA as matrix. (b) SALDI mass spectrum of AAP tablet measured with CHCA/HM20.

Figure 2a shows the MALDI mass spectrum of a fingerprint taken 4 h after ingesting the AAP tablet. As CHCA was used as the matrix, the peaks of  $H^+$  and  $Na^+$  adducted CHCA were observed. However, their intensities were weak, and peaks assignable to the ingredients in the tablet were not observed at all. This is probably because many impurities in the fingerprint suppressed the ionization of CHCA and the ingredients in the AAP tablet. A peak with an almost equal intensity to the CHCA peak was observed at  $m/z = 172$ , but

its origin is unknown. This peak at  $m/z = 172$  was also observed in Figure 1b, and was probably attributed to CHCA.

**Table 1.**  $m/z$  value, assignment, and intensity for each peak observed in Figure 1.

Observed Mass	Assignment	$I_{\text{CHCA}}$	$I_{\text{zeolite}}$	$I_{\text{zeolite}}/I_{\text{CHCA}}$
74.19		7340	2986	0.41
130.32		1062	3141	2.96
146.22		566	4026	7.11
149.22		4272	12,898	3.02
151.23		2804	1670	0.60
152.33	[AAP+H] <sup>+</sup>	13,004	14,815	1.14
166.25	[Eth+H] <sup>+</sup>	31,847	49,214	1.55
167.26		8630	21,197	2.46
172.20		2915	27,717	9.51
188.22		10,301	582	0.06
190.22	[CHCA+H] <sup>+</sup>	3919	31,118	7.94
195.25	[Caf+H] <sup>+</sup>	20,518	46,772	2.28
212.20	[CHCA+Na] <sup>+</sup>	13,954	1765	0.13
228.18		1904	87	0.05
234.19		3389	27	0.01
294.25		925	11,118	12.02
304.45		1267	19	0.01
335.29		341	2029	5.95



**Figure 2.** (a) MALDI and (b) SALDI mass spectra of fingerprint taken 4 h after ingesting AAP tablet.

The situation where chemical species in fingerprint could not be observed well by MALDI mass measurement using CHCA was dramatically improved by using the zeolite surface. Figure 2b shows the SALDI mass spectrum measured using CHCA/HM20. The use of zeolite significantly enhanced the peaks related to CHCA. Furthermore, some peaks assignable to chemical species in the fingerprint could be observed. For example, the peak of protonated urea,  $[\text{urea}+\text{H}]^+$ , was observed at  $m/z = 61$ , and is evidence of excretion from the fingertip [15]. As a peak related to the drug contained in the tablet, the GAAP peak was observed at  $m/z = 328$  as a proton adducted ion, albeit weakly at this magnification. Unknown peaks were observed at  $m/z = 234$  and 250. As the intensities of these peaks were as strong as that of CHCA peak, it seems unlikely that these peaks are due to the drug in the fingerprint or its metabolite.

The peaks of protonated AAP, Eth, Caf, and GAAP in Figure 2b are enlarged and displayed in Figure 3. The results of MALDI mass measurement using CHCA only as the matrix are also shown for comparison. The peaks of the above-mentioned chemical species in the fingerprint were observed for the first time by using SALDI with zeolite support even though their intensities were low. It is known that Eth contained in the tablet is converted into Sala by hydrolysis. As the molecular weight of Sala is 137, the peak of protonated Sala should be observed at  $m/z = 138$  if Sala is present in the fingerprint. In fact, a peak thought to be derived from protonated Sala was observed at  $m/z = 138$ , as shown in Figure 3j. Regarding the strong peak of  $m/z = 139$  observed in Figure 2, it may be possible to consider that this was a peak of proton-adducted salicylic acid (Sal). As the acetaminophen tablets taken by the subjects do not contain Sal, it should be considered that Sal was produced by metabolism. However, it is noted that the peak intensity of  $m/z = 139$  was strong and that it did not show a clear time dependence, as shown later in Figure 5 (Figure S1). Peaks shown in Figure 3, the peak at  $m/z = 139$  in Figure 2 and the deviations from the accurate mass, are summarized in Table 2.

**Table 2.** Peaks shown in Figure 3 and the deviations from the accurate mass.

Species	Molecular Weight	Observed Ion	Accurate Mass	Observed Mass	Deviation
AAP	151.17	$[\text{AAP}+\text{H}]^+$	152.17	152.10	−0.07
Eth	165.19	$[\text{Eth}+\text{H}]^+$	166.19	166.12	−0.07
Caf	194.19	$[\text{Caf}+\text{H}]^+$	195.19	195.11	−0.08
GAAP	327.29	$[\text{GAAP}+\text{H}]^+$	328.29	328.05	−0.24
Sal	138.12	$[\text{Sal}+\text{H}]^+$	139.12	139.11	−0.01
Sala	137.14	$[\text{Sala}+\text{H}]^+$	138.14	138.11	−0.03

A schematic diagram of drug metabolism in the human body is shown in Figure 4. A drug is metabolized by the liver and excreted into the bile by oral administration. Most drugs undergo oxidation by CYP450 (hepatic cytochrome CYP450 enzyme) in the liver (phase I reaction), followed by a conjugation reaction (phase II reaction) to become water-soluble, and are excreted with bile into the intestinal tract. In the phase I reaction, the drug undergoes oxidation, reduction, and hydrolysis to make it more soluble in water. In the phase II reaction, water-soluble substances, such as glucuronic acid, amino acids, and sulfuric acid, are attached to make the drug soluble in water. The conversion of Eth into Sala observed in Figure 3j corresponds to the phase I reaction. A phase I reaction followed by a phase II reaction transforms AAP into its glucuronide conjugate (GAAP). This change was confirmed by the detection of GAAP excretion into the fingerprint, as shown in Figure 3h.

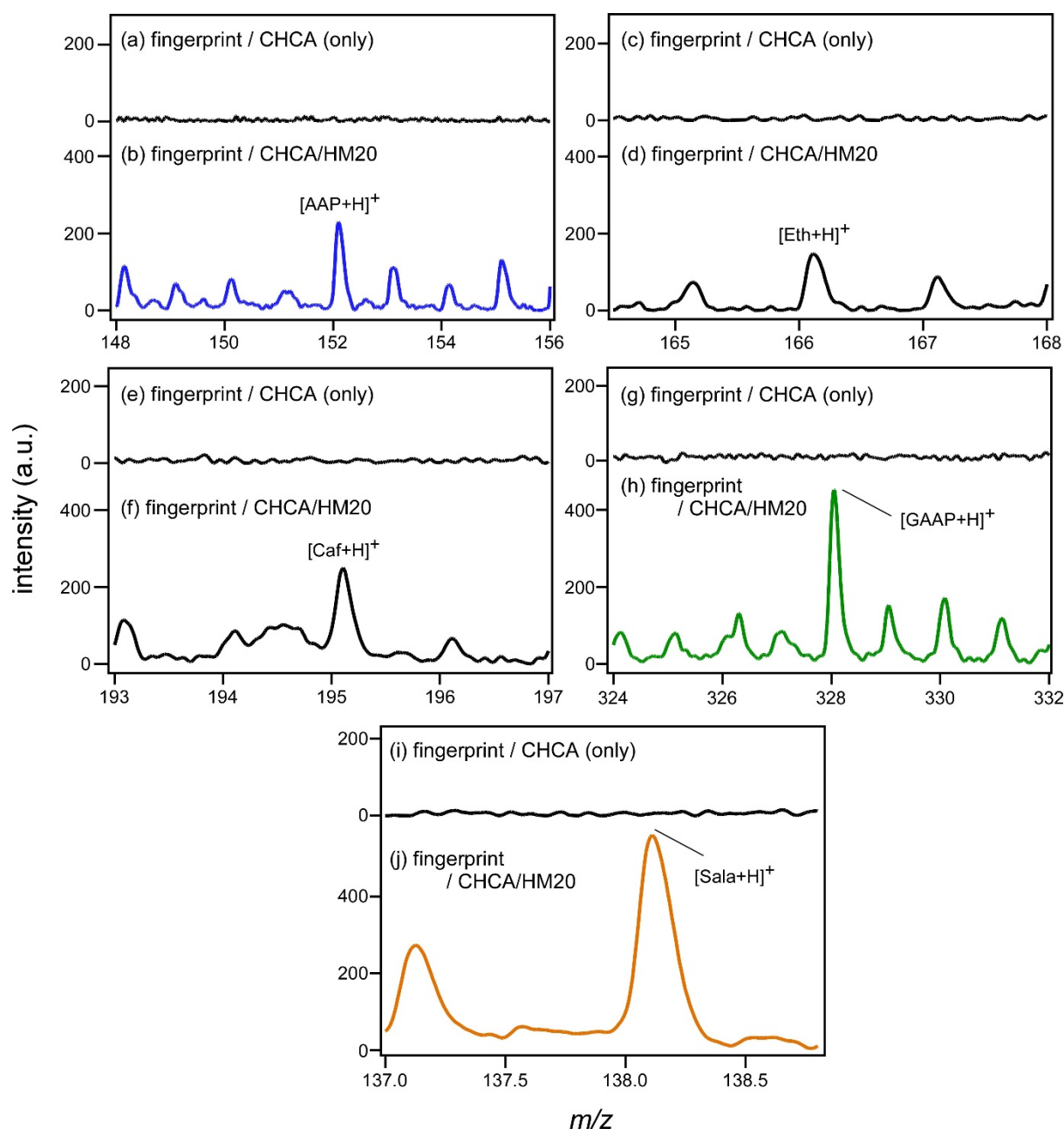


**Figure 3.** Enlarged view of Figure 2a,b in the mass region related to the ingredients in AAP tablet and AAP metabolite.

Figures 2 and 3 show the mass spectra of fingerprint obtained 4 h after ingestion of an AAP tablet. In order to investigate drug excretion and metabolism, mass spectra were measured at various times after ingestion; the time dependence of the peak intensities of  $[AAP+H]^+$  and  $[GAAP+H]^+$  is shown in Figure 5. The results in Figure 5 are the average of  $N = 3$  measurements, and the standard deviations are shown as error bars. The results could be reproduced by double exponential functions convoluted with a Gaussian line profile as the response function. Here, the fitting was performed assuming that the response function by the human body was 1 h ( $\Delta = 1$  h). The reaction rate constants ( $\text{hour}^{-1}$ ) for the rise and decay components are  $k_{\text{rise}} = 0.72 \pm 0.25$  and  $k_{\text{decay}} = 0.32 \pm 0.14$  for the peak intensity of  $[AAP+H]^+$ , and  $k_{\text{rise}} = 1.8 \pm 0.25$  and  $k_{\text{decay}} = 0.33 \pm 2.6$  for the peak intensity of  $[GAAP+H]^+$ , respectively. It can be seen that the increase of  $[GAAP+H]^+$  peak started later than that of  $[AAP+H]^+$  peak, although the rise time constant for GAAP is larger than that for AAP. In fact, the time intercepts for both time profiles were determined by the



fitting analysis and were 1.1 h for  $[AAP+H]^+$  and 1.9 h for  $[GAAP+H]^+$  after ingestion of the drug. In other words, because it took time to metabolize AAP into GAAP in the body, the time until the appearance of  $[GAAP+H]^+$  was delayed. Nevertheless,  $[GAAP+H]^+$  showed a fast rise, and both  $[AAP+H]^+$  and  $[GAAP+H]^+$  reached maximum concentrations at approximately 3 h after ingestion. It could also be seen that the decay of both species was approximately  $0.3 \text{ (h}^{-1}\text{)}$ . This means that AAP and GAAP were excreted from the body with a half-life of approximately 3.3 h. The measurement was performed only up to 6 h after ingestion. However, extrapolation of the figure revealed that the excretion of both components would be almost completed 8 h after ingestion. In Figure 5b, the value of  $[AAP+H]^+ / [GAAP+H]^+$  was also depicted. It was confirmed that the amount of AAP decreased single exponentially compared with that of GAAP, reflecting the metabolism of AAP. For other metabolites of AAP, however, the time change as shown in Figure 5 could not be measured due to the unstable observation of peaks.

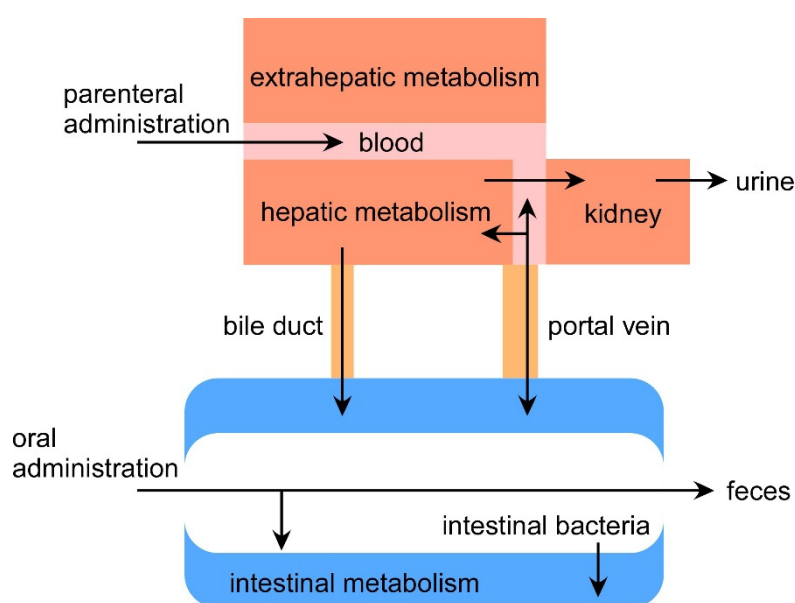


**Figure 4.** Schematic diagram of drug metabolism in the human body.

Finally, we would like to discuss fingerprint recovery. Mass spectrometry is unsuitable for fingerprint measurement because it destroys the sample, which, in this case, is fingerprint that serves as important forensic evidence, during measurement. Figure 6 shows the optical micrographs of portions of fingerprints. It should be noted that these are not the fingerprints measured in this mass spectrometric study. Figure 6a shows an image of an unprocessed fingerprint. The white stripes of the fingerprint are visible, although the stripes are not clear. Figure 6b is an image of a fingerprint visualized with activated carbon. Activated carbon adheres to sweat and fat components in the fingerprint, making it easier to see the striped pattern. In Figure 6c, CHCA/HM20 was applied to the fingerprint used in Figure 6a and dried. Generally, fingerprint powder contains silica in addition to aluminum or magnetic particles. HM20, which is used as a material to support CHCA, is an aluminosilicate, and is thus expected to play the same role as silica in fingerprint powder. In fact, compared with Figure 6b, the image was clearer when CHCA/HM20 was applied. Note that activated carbon was not used in Figure 6c. Figure 6d–f are fingerprint images after laser irradiation. From Figure 6d, it was confirmed that the fingerprint shape remained distinct even after CHCA/HM20 was washed off after laser irradiation for 30 s. However, the fingerprint shape became unclear when the laser irradiation time was increased to 1 or 5 min. Of course, this situation would also be affected by the method of washing off CHCA/HM20, the amount of solvent, and the laser power. Here, the fingerprints from Figure 6d–f were washed in the same way with 10 mL of solvent. The laser power is

18  $\mu\text{J}$ , which is approximately three times the power used in mass measurements. The wavelength used is 266 nm, which is also different from the wavelength used in the mass measurement in this study. In actual mass measurements, the laser irradiation time was 20 s (200 shots in 10 Hz operation), and the laser power used was sufficiently low (5.9  $\mu\text{J}$ ). The results in Figure 6 were obtained under fairly severe conditions. As the fingerprints are preserved even under such conditions, we can say that forensic evidence is preserved after mass measurements.

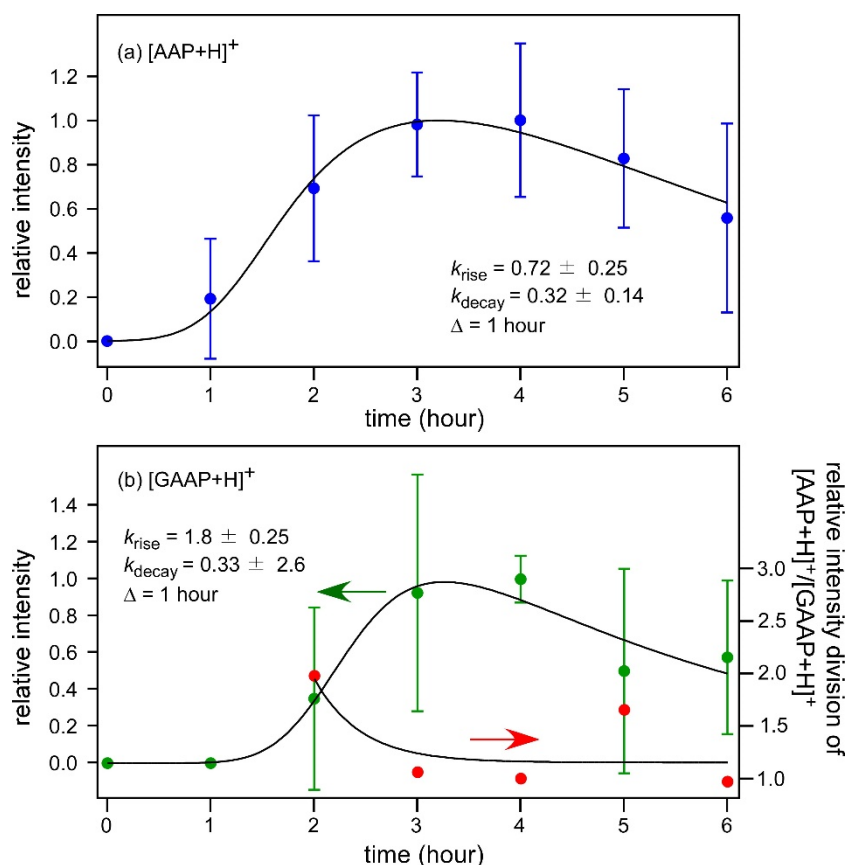


**Figure 5.** Time dependence of peak intensities of (a)  $[\text{AAP}+\text{H}]^+$  and (b)  $[\text{GAAP}+\text{H}]^+$ . Relative intensity division of  $[\text{AAP}+\text{H}]^+ / [\text{GAAP}+\text{H}]^+$  was also shown in (b).

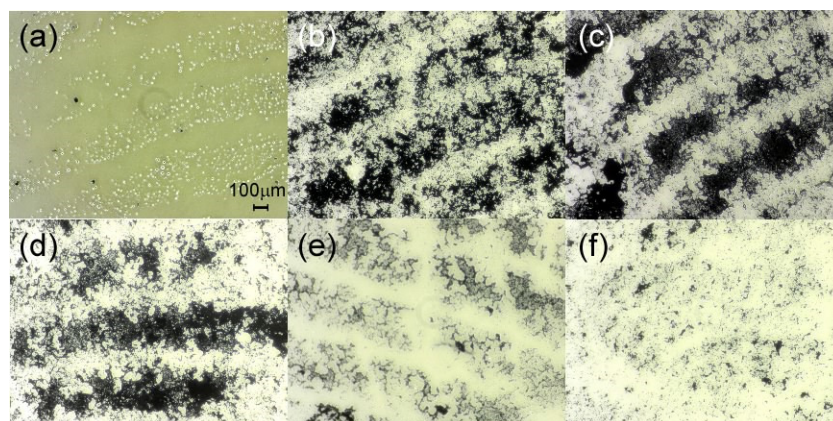


**Figure 6.** Optical micrographs of (a) unprocessed fingerprint, (b) fingerprint with activated carbon powder, and (c) fingerprint with CHCA/HM20. Images of fingerprint after laser irradiation for (d) 30 s, (e) 1 min, and (f) 5 min.



#### 4. Conclusions

The ingredients in AAP tablet and their metabolites excreted into fingerprints were detected by SALDI mass spectrometry using CHCA/HM20. Fingerprints were collected from multiple volunteers who ingested commercially available AAP tablet due to such symptoms as headache. All volunteers took the same tablet composed mainly of AAP, Eth, and Caf. In the fingerprint taken 4 h after ingestion, AAP, Caf, and Eth were detected as proton adducted ions. GAAP and Sala were also detected as the metabolites of AAP and Eth, respectively. Fingerprints were collected over time to determine how the amounts of drug and its metabolite change with time, and the time dependence of the peak intensities of protonated AAP and GAAP was measured. It was found that the increase of [GAAP+H]<sup>+</sup> peak started later than that of [AAP+H]<sup>+</sup> peak, reflecting the metabolism of AAP. It was also found that both AAP and GAAP reached maximum concentrations approximately 3 h after ingestion and were excreted from the body with a half-life of approximately 3.3 h; the  $k_{decay}$  was  $0.32 \pm 0.14$  and  $0.33 \pm 2.6$  for AAP and GAAP, respectively. In addition, the application CHCA/HM20 on fingerprints enabled fingerprint preservation, as confirmed by optical microscopy. The fingerprint shape could be sufficiently retained without being destroyed by laser irradiation for 1 min under our experimental conditions. Our method may be used in fingerprint analysis.

**Supplementary Materials:** The following are available online at <https://www.mdpi.com/article/10.3390/analytica2030008/s1>, Figure S1: Time dependence of peak intensity at  $m/z = 139$ .

**Author Contributions:** T.H., C.K., Y.F., J.X. and T.F. performed the experiments, analyzed the data, and contributed reagents/materials/analysis tools. T.A. and T.F. conceived and designed the experiments. T.F. wrote the paper. All authors have read and agreed to the published version of the manuscript.

**Funding:** This work was partly supported by the research program “Network Joint Research Center for Materials and Devices”, Japan.

**Institutional Review Board Statement:** Not applicable.

**Informed Consent Statement:** Informed consent was obtained from all subjects involved in the study.

**Conflicts of Interest:** The authors declare that there are no competing interests and ethics problems.

#### References

1. Sodhi, G.S.; Kaur, J. Powder method for detecting latent fingerprints: A review. *Forensic Sci. Int.* **2001**, *120*, 172–176. [[CrossRef](#)]
2. King, R.S.; Hallett, P.M.; Foster, D. Seeing into the infrared: A novel IR fluorescent fingerprint powder. *Forensic Sci. Int.* **2015**, *249*, e21–e26. [[CrossRef](#)] [[PubMed](#)]
3. Hazarika, P.; Jickells, S.M.; Wolff, K.; Russell, D.A. Imaging of Latent Fingerprints through the Detection of Drugs and Metabolites. *Angew. Chem. Int. Ed.* **2008**, *47*, 10167–10170. [[CrossRef](#)] [[PubMed](#)]
4. Hazarika, P.; Russell, D.A. Advances in Fingerprint Analysis. *Angew. Chem. Int. Ed.* **2012**, *51*, 3524–3531. [[CrossRef](#)] [[PubMed](#)]
5. Archer, N.E.; Charles, Y.; Elliott, J.A.; Jickells, S. Changes in the lipid composition of latent fingerprint residue with time after deposition on a surface. *Forensic Sci. Int.* **2005**, *154*, 224–239. [[CrossRef](#)] [[PubMed](#)]
6. Mountfort, K.A.; Bronstein, H.; Archer, N.; Jickells, S.M. Identification of Oxidation Products of Squalene in Solution and in Latent Fingerprints by ESI-MS and LC/APCI-MS. *Anal. Chem.* **2007**, *79*, 2650–2657. [[CrossRef](#)] [[PubMed](#)]
7. Jacob, S.; Jickells, S.; Wolff, K.; Smith, N. Drug Testing by Chemical Analysis of Fingerprint Deposits from Methadone-Maintained Opioid Dependent Patients Using UPLC-MS/MS. *Drug Metab. Lett.* **2008**, *2*, 245–247. [[CrossRef](#)] [[PubMed](#)]
8. Bumrah, G.S.; Sharma, R.M.; Jasuja, O.P. Emerging latent fingerprint technologies: A review. *Res. Rep. Forensic Med. Sci.* **2016**, *6*, 39–50. [[CrossRef](#)]
9. Yang, H.; Li, S.; Zhang, Q.; Wang, Z.; Li, N.; Han, C.; Huo, Q.; Zhao, Z. Combination of electrospray deposition technology of TiO<sub>2</sub> nanoparticles and MALDI FTICR MSI for identification of fingerprint morphology and latent components. *Talanta* **2019**, *198*, 310–315. [[CrossRef](#)] [[PubMed](#)]
10. Scotcher, K.; Bradshaw, R. The analysis of latent fingermarks on polymer banknotes using MALDI-MS. *Sci. Rep.* **2018**, *8*, 8765. [[CrossRef](#)] [[PubMed](#)]
11. Amin, M.O.; Madkour, M.; Al-Hetlani, E. Metal oxide nanoparticles for latent fingerprint visualization and analysis of small drug molecules using surface-assisted laser desorption/ionization mass spectrometry. *Anal. Bioanal. Chem.* **2018**, *410*, 4815–4827. [[CrossRef](#)] [[PubMed](#)]

12. Ifa, D.R.; Manicke, N.E.; Dill, A.L.; Cooks, R.G. Latent Fingerprint Chemical Imaging by Mass Spectrometry. *Science* **2008**, *321*, 805. [[CrossRef](#)] [[PubMed](#)]
13. Wolstenholme, R.; Bradshaw, R.; Clench, M.R.; Francese, S. Study of latent fingerprints by matrix-assisted laser desorption/ionisation mass spectrometry imaging of endogenous lipids. *Rapid Commun. Mass Spectrom.* **2009**, *23*, 3031–3039. [[CrossRef](#)] [[PubMed](#)]
14. Kitaoka, C.; Asano, T.; Fujino, T. Direct Measurement and Quantification of Drugs and Their Metabolites in Urine by MALDI-MS Using Zeolite. *Bull. Chem. Soc. Jpn.* **2017**, *90*, 154–160. [[CrossRef](#)]
15. Schwartz, I.L.; Thaysen, I.H.; Dole, V.P. Urea excretion in human sweat as a tracer for movement of water within the secreting gland. *J. Exp. Med.* **1953**, *97*, 429–437. [[CrossRef](#)] [[PubMed](#)]